

Modeling and Simulation of the i.e.

Methanol Fuel Cell

M. Wohr

German Aerospace Research Establishment e.V. (DLR)
Institute of Technical Thermodynamics
Maffenwaldweg, 38-40, D-70569 Stuttgart, Germany

S.R. Narayanan and G. Halpert
Jet Propulsion Laboratory,
California Institute of Technology
4800 Oak Grove Drive, Pasadena, CA 91109

INTRODUCTION

The direct methanol liquid feed fuel cell uses aqueous solutions of methanol as fuel and oxygen or air as the oxidant and uses an ionically conducting polymer membrane such as Nafion[®] as the electrolyte [1-3]. This type of direct oxidation cell is fuel versatile and offers significant advantages in terms of simplicity of design and operation. In order to improve the performance of these cells, it is necessary to model the various phenomena occurring in these cells. The present study focuses on the results of a phenomenological model based on current understanding of the various processes operating in these cells.

MODELING APPROACH

The model is based on liquid feed methanol fuel cells which use (i) high volume fractions of recast Nafion and little void volume fractions in the catalytic layers; (ii) Pt-Ru and Pt as catalysts on the anode and cathode side, respectively; (iii) Nafion[®] as separator; and (iv) low operating temperatures (60-90°C). The assumptions of the model are as follows: (i) polymer in anodic reaction layer and separator can be assumed to be fully hydrated even at high current densities; (ii) transport of methanol at the anode side occurs only in the solution phase; (iii) no concentration gradient of water exists across the separator membrane; (iv) only electroosmotic forces move water through the membrane; (v) for methanol transport, migration and diffusion are considered; (vi) on the cathode side, oxygen and methanol transport is considered in narrow gas pores and in solution phase and Henry's law is obeyed [4,5]; (vi) in the cathodic reaction layer, the gas volume fraction decreases with increasing water content.

The model equations are time dependent but at present only steady state results have been obtained.

RESULTS

At low current densities, reaction occurs uniformly throughout anode and cathode reaction layers. At high current densities, most of the reaction takes place

close to the backing layer due to diffusion limitation of reactant species, this results in higher ohmic losses and higher overpotentials due to lower concentrations. On the anode side, comparison of simulation results and experimental data shows additional diffusion losses in the backing layer. This results in losses of the anode performance but on the other hand, methanol crossover is decreased due to lower concentrations. Calculations show that most of the methanol crossover results due to diffusion, even at 600mA/m², migration contribution to mass transport is small. Nevertheless, including electroosmotic forces in the model results in better agreement between experimental data and simulation results, especially at high methanol concentrations. On the cathode side, comparison of simulation results and experimental data shows a decrease of gas volume fraction at higher current densities because of partial flooding of the catalytic layer. Due to high cathode potentials, methanol which crosses to the cathode side, reacts immediately after entering the catalytic layer. At low current densities, the oxygen reduction reaction occurs uniformly throughout the reaction layer, whereas at higher current densities, almost all the oxygen reacts close to the backing layer, thereby resulting in almost complete spatial separation of the two reactions.

ACKNOWLEDGEMENTS

The authors are thankful to the California Institute of Technology for providing the facilities to work, to Paul Timmerman, B.V. Ratnakumar, A. Kindler of the Jet Propulsion Laboratory and George Gavalas of the California Institute of Technology for useful discussions.

REFERENCES

1. S. Surampudi, S. R. Narayanan, E. Vamoss, H. Frank and G. Halpert, *J. Power Sources*, **47**, 377-385 (1994)
2. S. R. Narayanan, A. Kindle, B. J. Nakamura, W. Chun, M. Smart, H. Frank and G. Halpert, *Proceedings of the First Symposium on Proton Conducting Fuel Cells*, Volume 95-23, p. 261 (1995)
3. S. R. Narayanan, H. Frank, B. J. Nakamura, W. Chun, M. Smart, G. Halpert, J. Kosick, G. G. Topley, *ibid*, p. 278 (1995)
4. D. Bernardi, M. Verbrugge, *J. Electrochem. Soc.*, **139**, 2477-2491 (1992)

Modeling and Simulation of the Direct Methanol Fuel Cell

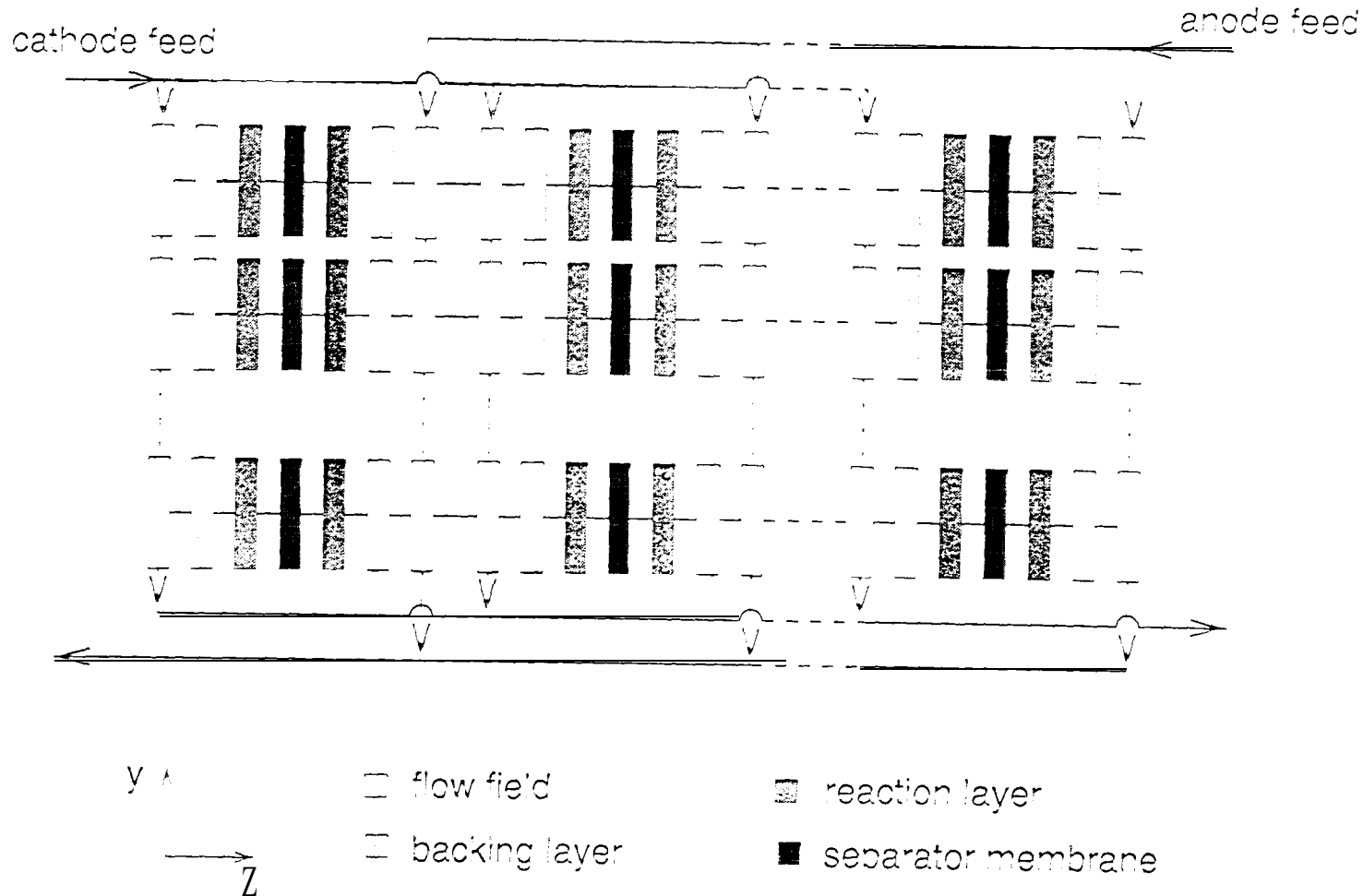
M. Wöhr
Deutsche Forschungsanstalt für Luft- und Raumfahrt e.V. (DLR)
Institut für Technische Thermodynamik
Stuttgart, Germany

S.R. Narayanan, G. Halpert
Jet Propulsion Laboratory (JPL)
California Institute of Technology (Caltech)
Pasadena, CA

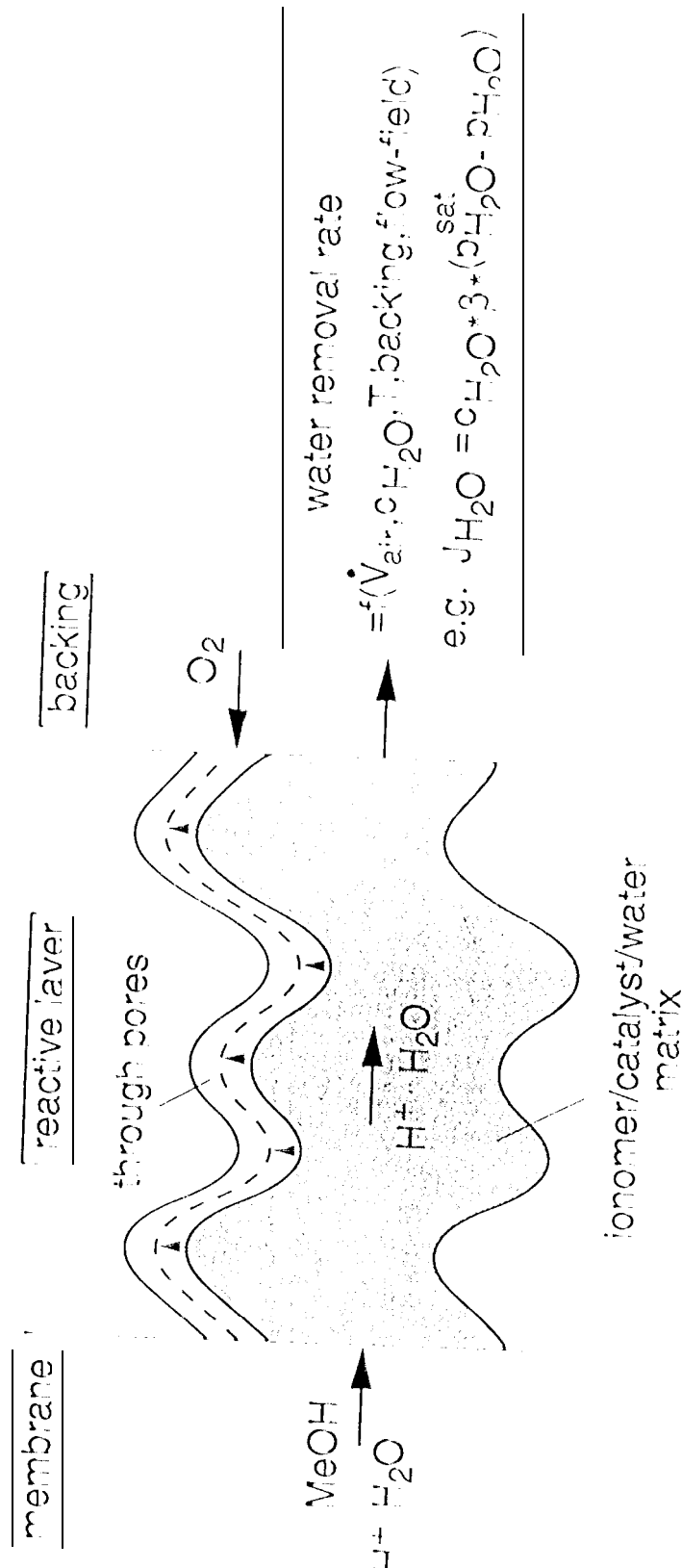
190th meeting of the Electrochemical Society - San Antonio, Texas



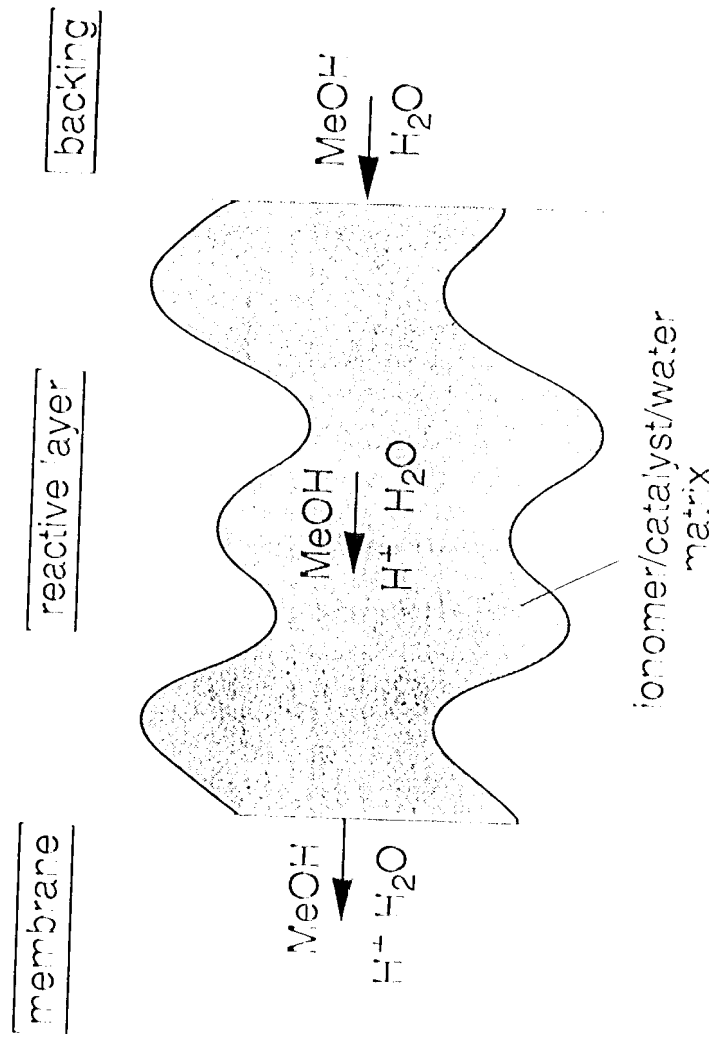
modular design of simulation process



modeling approach of electrode on cathode side



modeling approach of electrode on anode side



modeling of mass transport in reactive layers

gas-phase species

$$-\frac{dp_j}{dz} - p_j \frac{B_0}{\eta_g D_j^g} \frac{dp}{dz} = RT \left(\frac{J_j^g}{\frac{\varepsilon_g}{\tau_g} D_j^g} + \sum_{i=1, i \neq j}^K \frac{p_i J_j^g - p_j J_i^g}{p \frac{\varepsilon_g}{\tau_g} D_{ij}^g} \right)$$

liquid water

$$J_w^i = -\frac{\varepsilon_l}{\tau_l} D_w^i \frac{dc_w}{dz} + \frac{3}{F} i_{H^+}$$

dissolved methanol

$$J_m^l = -\frac{\varepsilon_l}{\tau_l} D_m^l \frac{dc_m}{dz} + \frac{c_m}{55.56} J_w^i$$

modeling of electrochemical reactions

reaction rate of oxygen reduction

$$j_1 = -a_s i_1^{\text{ref1}} \exp\left(\frac{-E_{a1}}{R}\left(\frac{1}{T} - \frac{1}{T_{\text{ref1}}}\right)\right) \frac{c_{O_2}}{c_{O_2}^{\text{ref1}}} \exp\left(\frac{2.3\eta_1}{b_1}\right)$$

reaction rate of methanol oxidation

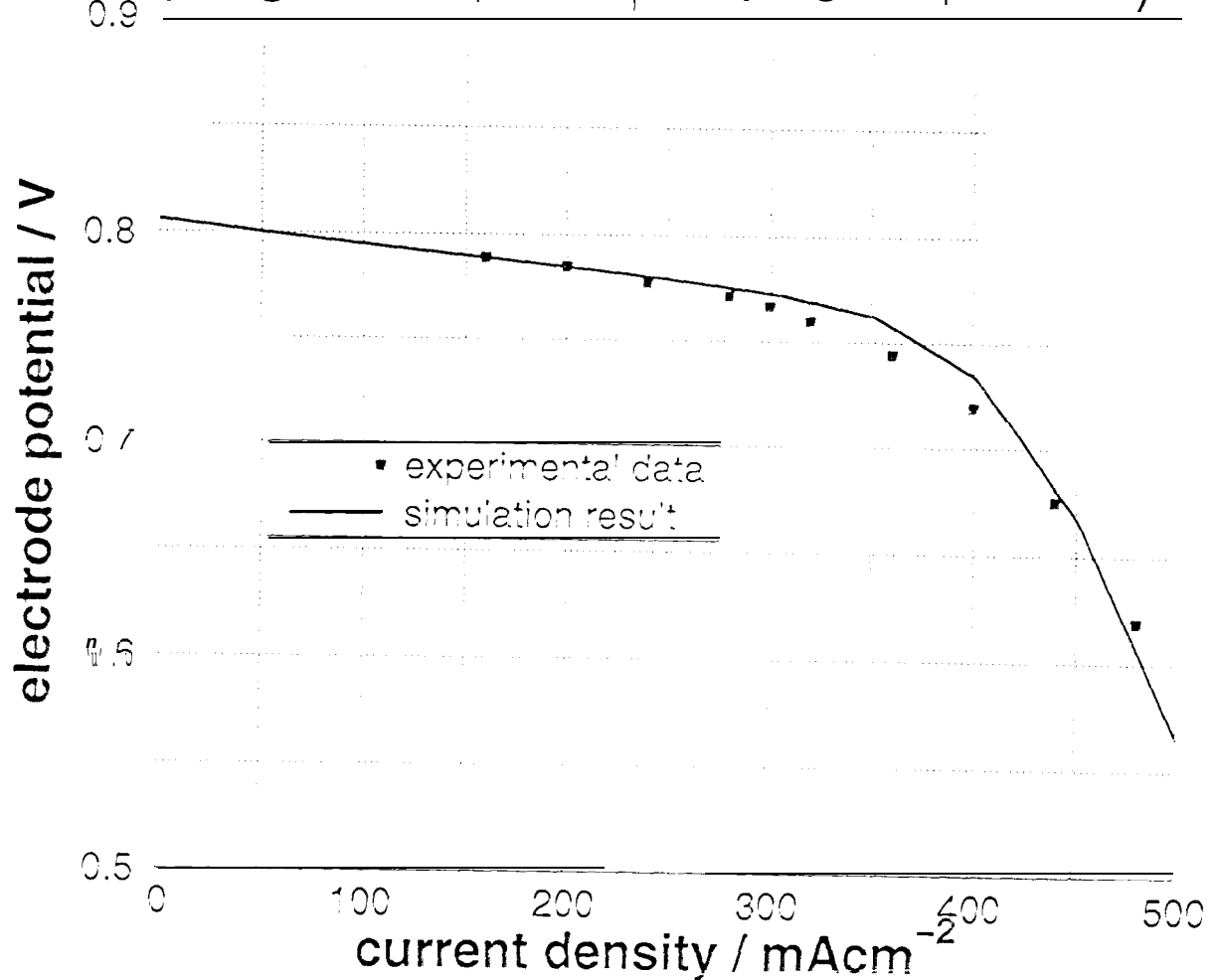
$$j_2 = a_s i_2^{\text{ref2}} \exp\left(\frac{-E_{a2}}{R}\left(\frac{1}{T} - \frac{1}{T_{\text{ref2}}}\right)\right) \frac{c_m}{c_m^{\text{ref2}}} \exp\left(\frac{2.3\eta_2}{b_2}\right)$$

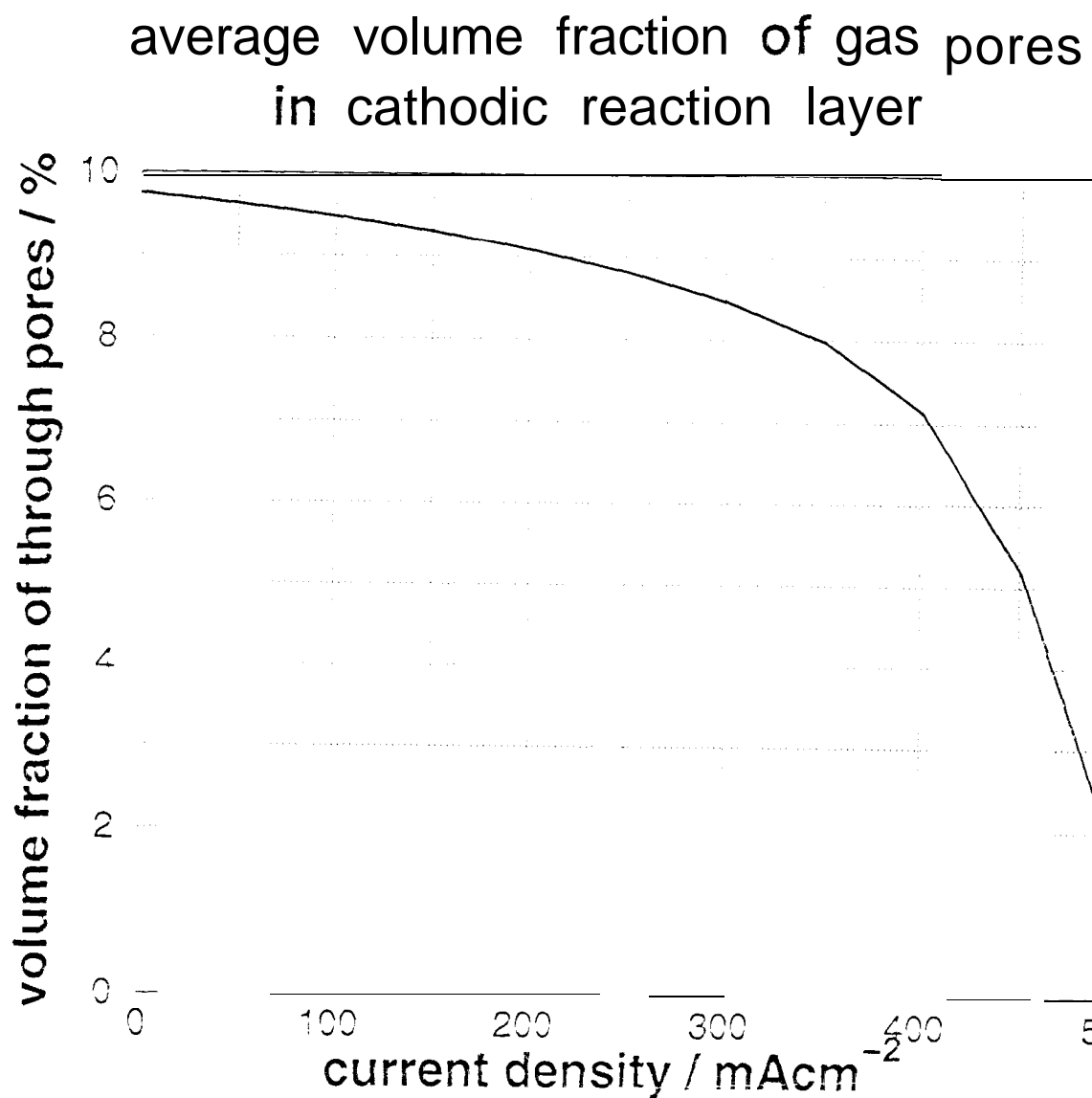
gradient of ionic current density

$$\frac{di_{H^+}}{dz} = j_1 + j_2$$

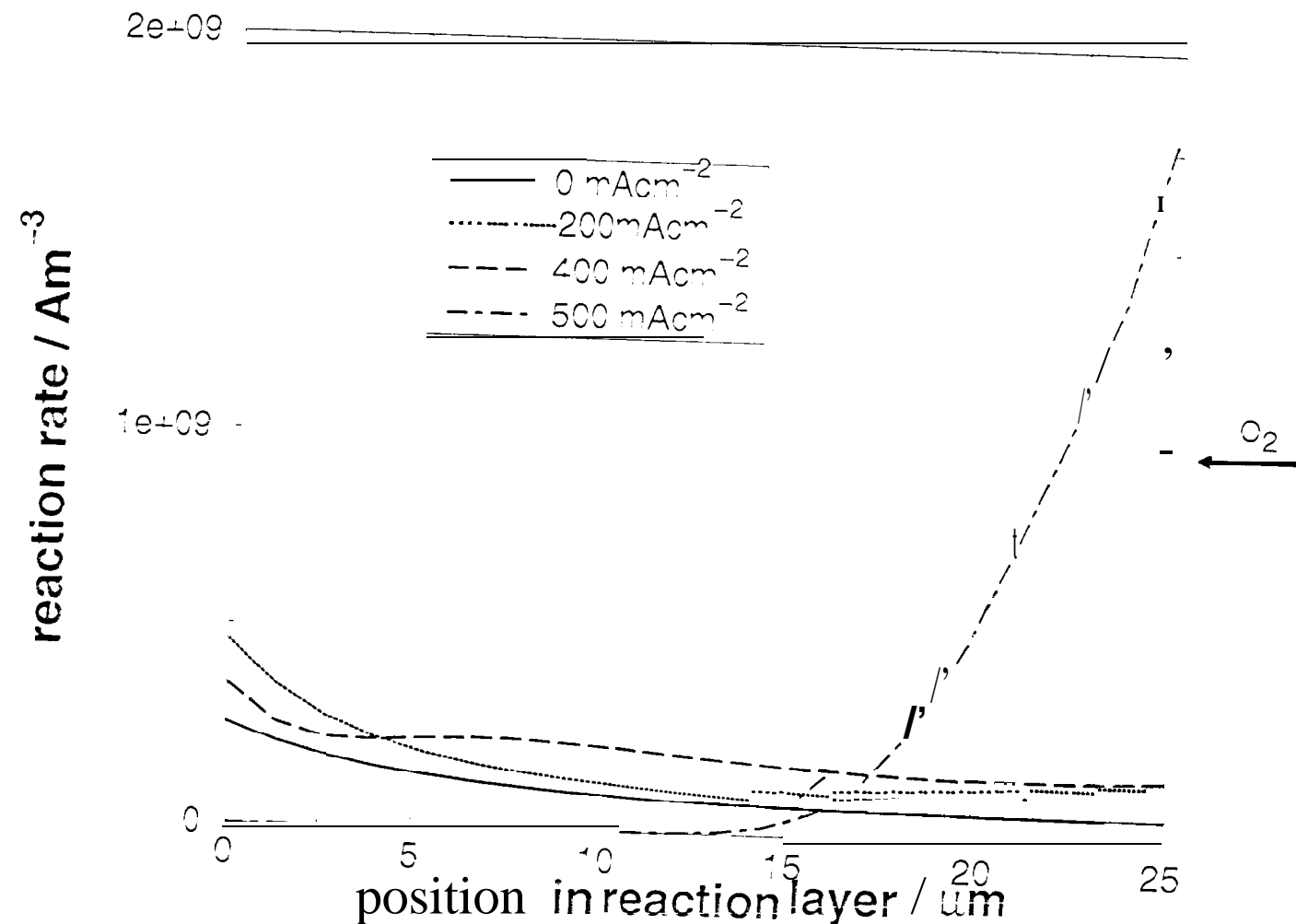
cathode performance - experiment / simulation

(4mgcm^{-2} Pt, 90°C, 20psig air, 1 l/min)

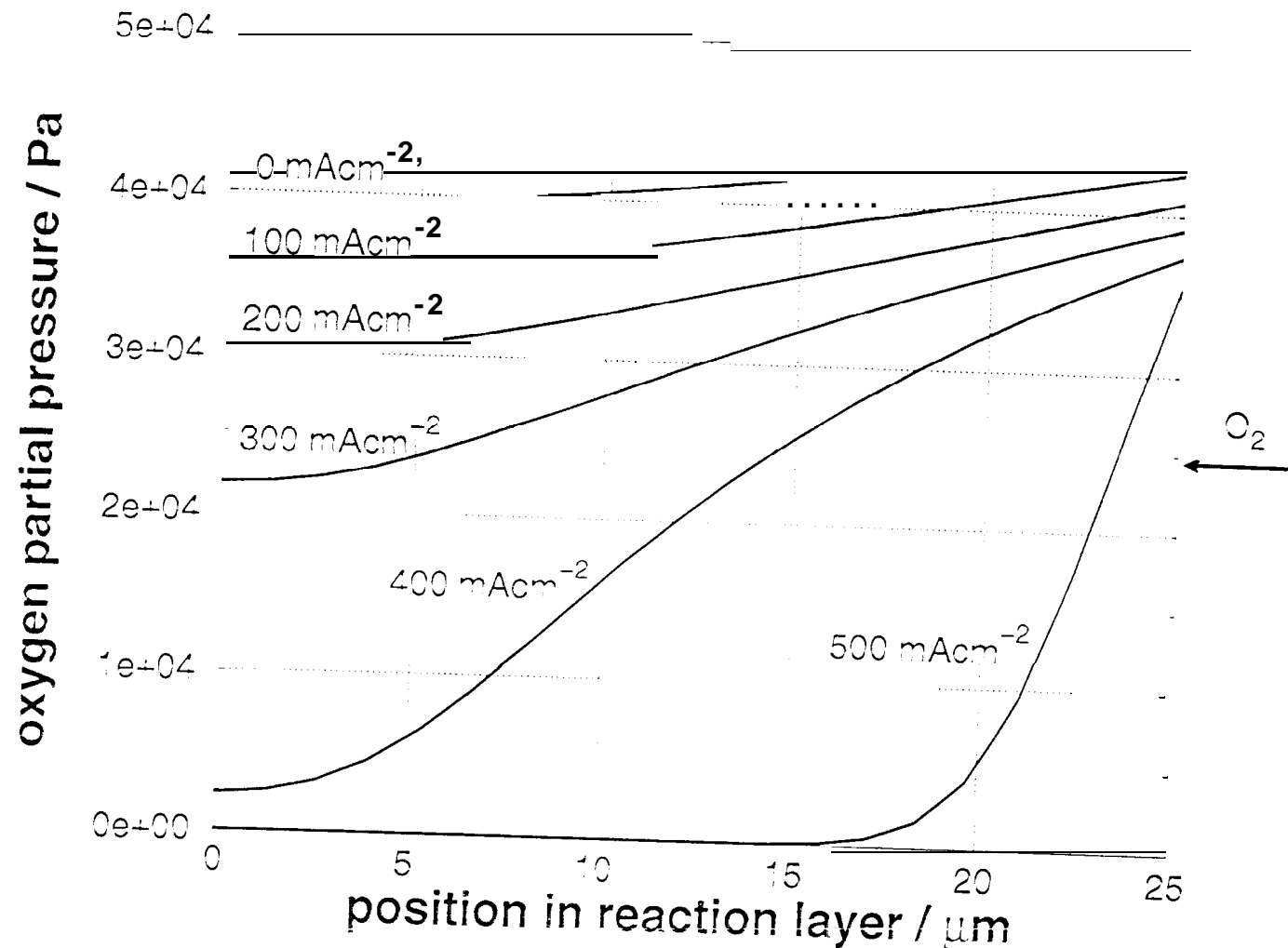




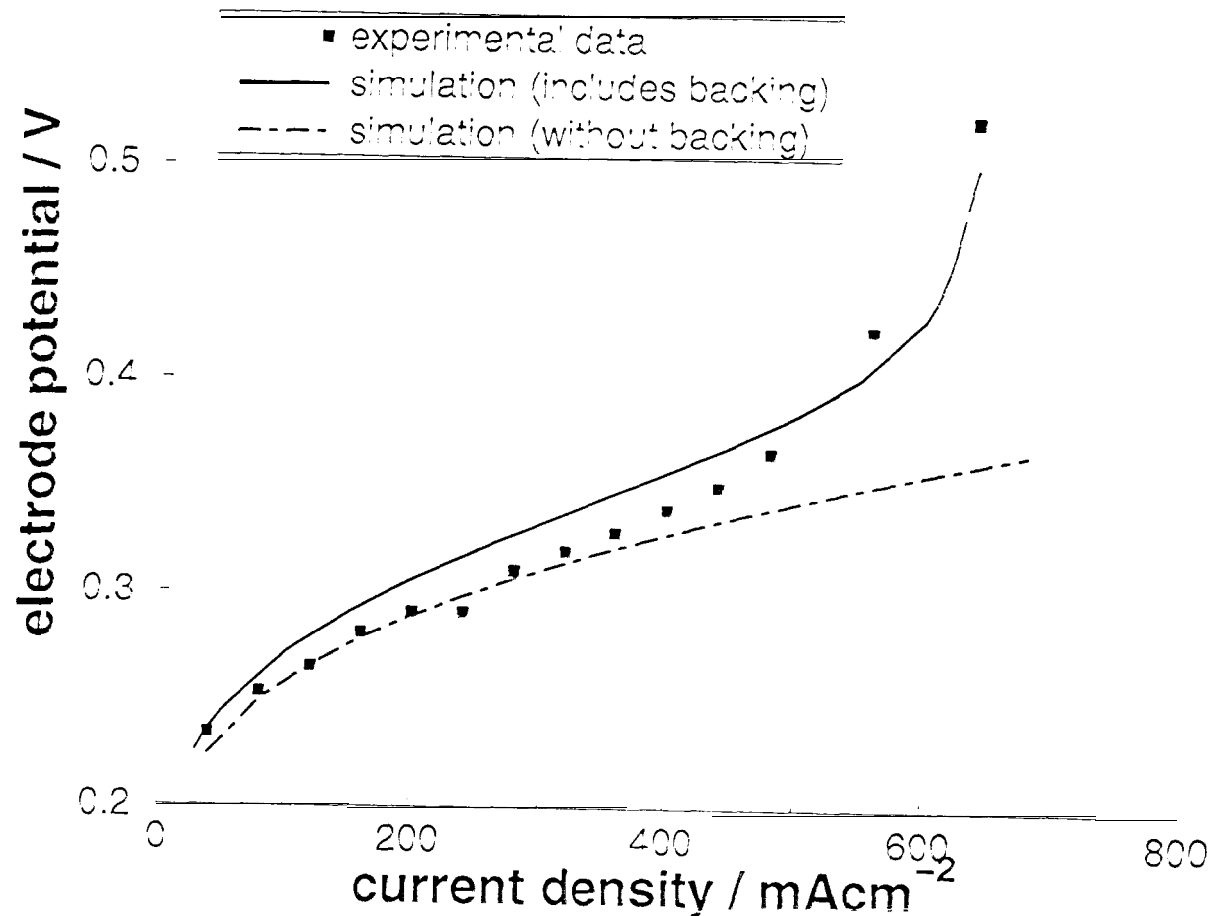
Distribution of reaction rate in cathodic reaction layer



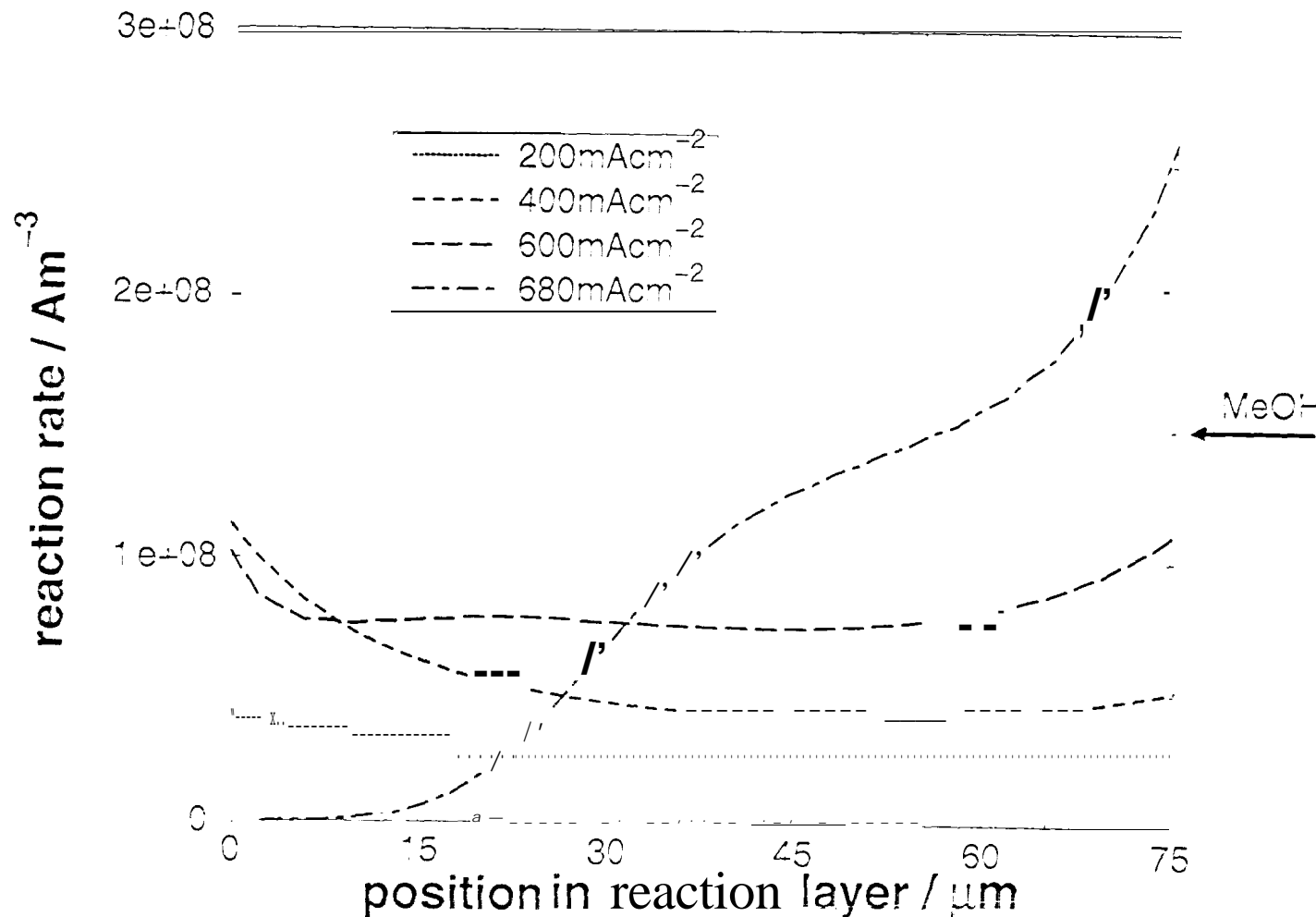
Distribution of oxygen concentration in cathodic reaction layer



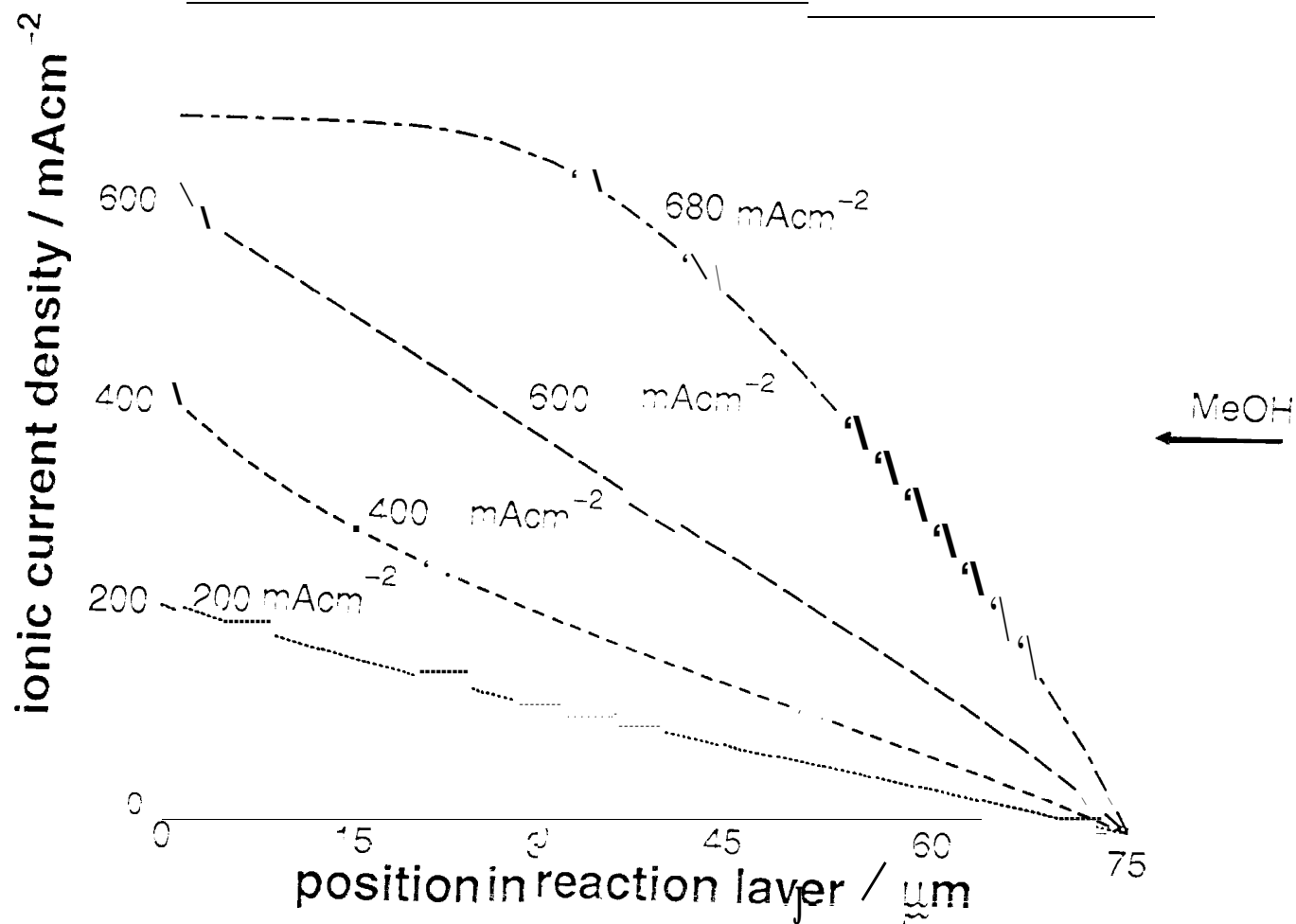
anode performance - experiment / simulation
(12 mgcm^{-2} Pt-Ru, 1 M MeOH, 90°C)



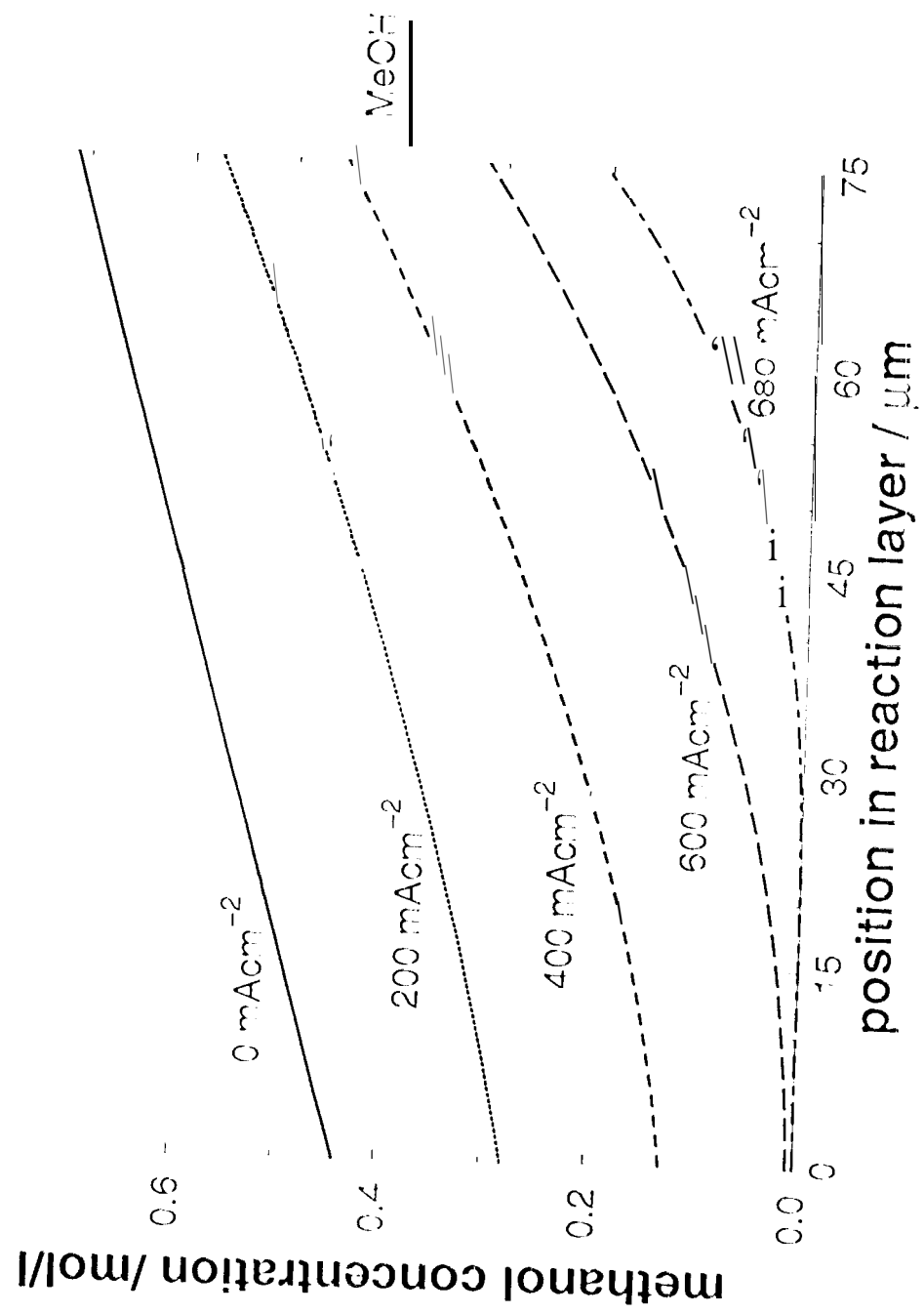
Distribution of reaction rate in anodic reaction layer



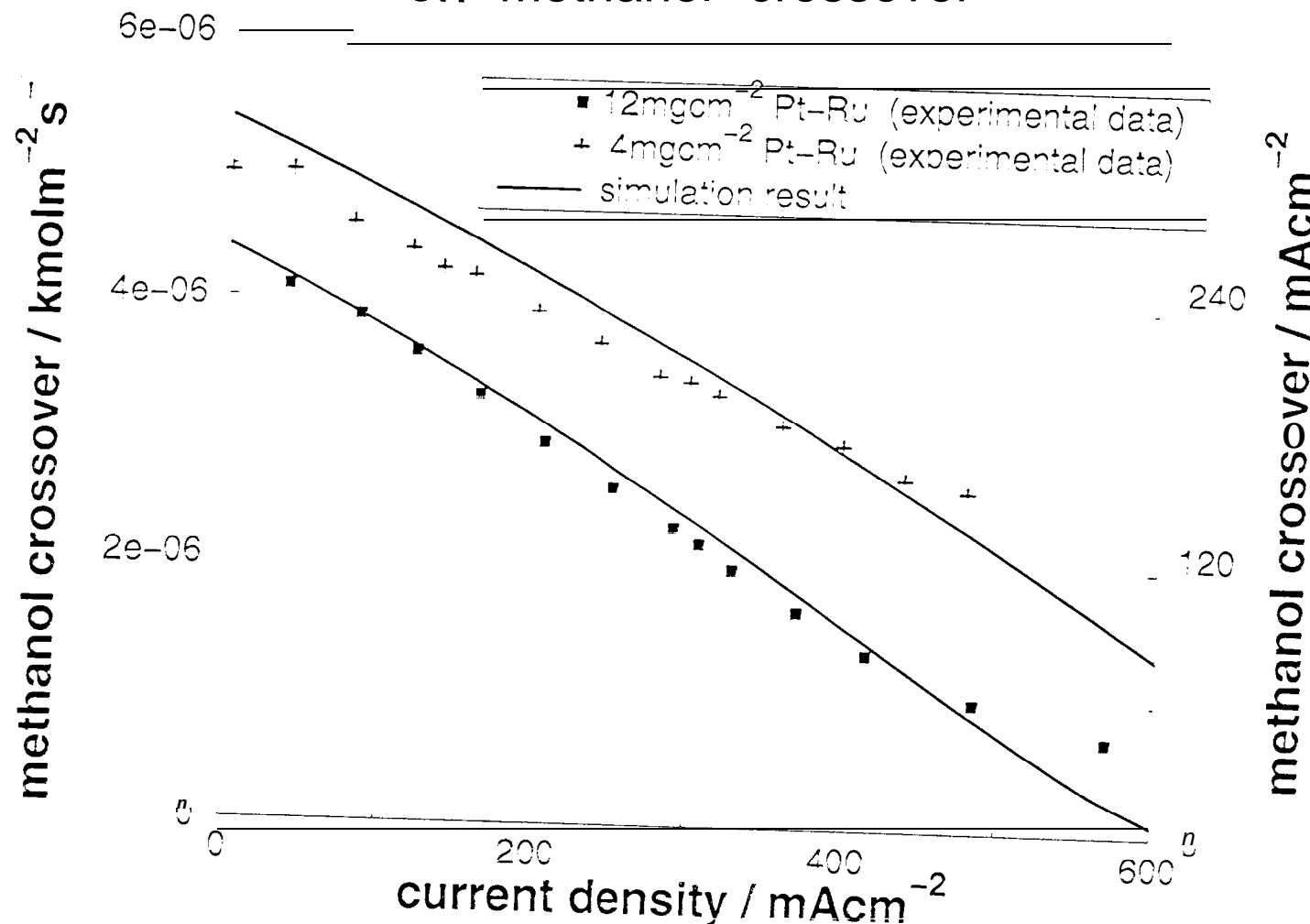
Distribution of ionic current density in anodic reaction layer



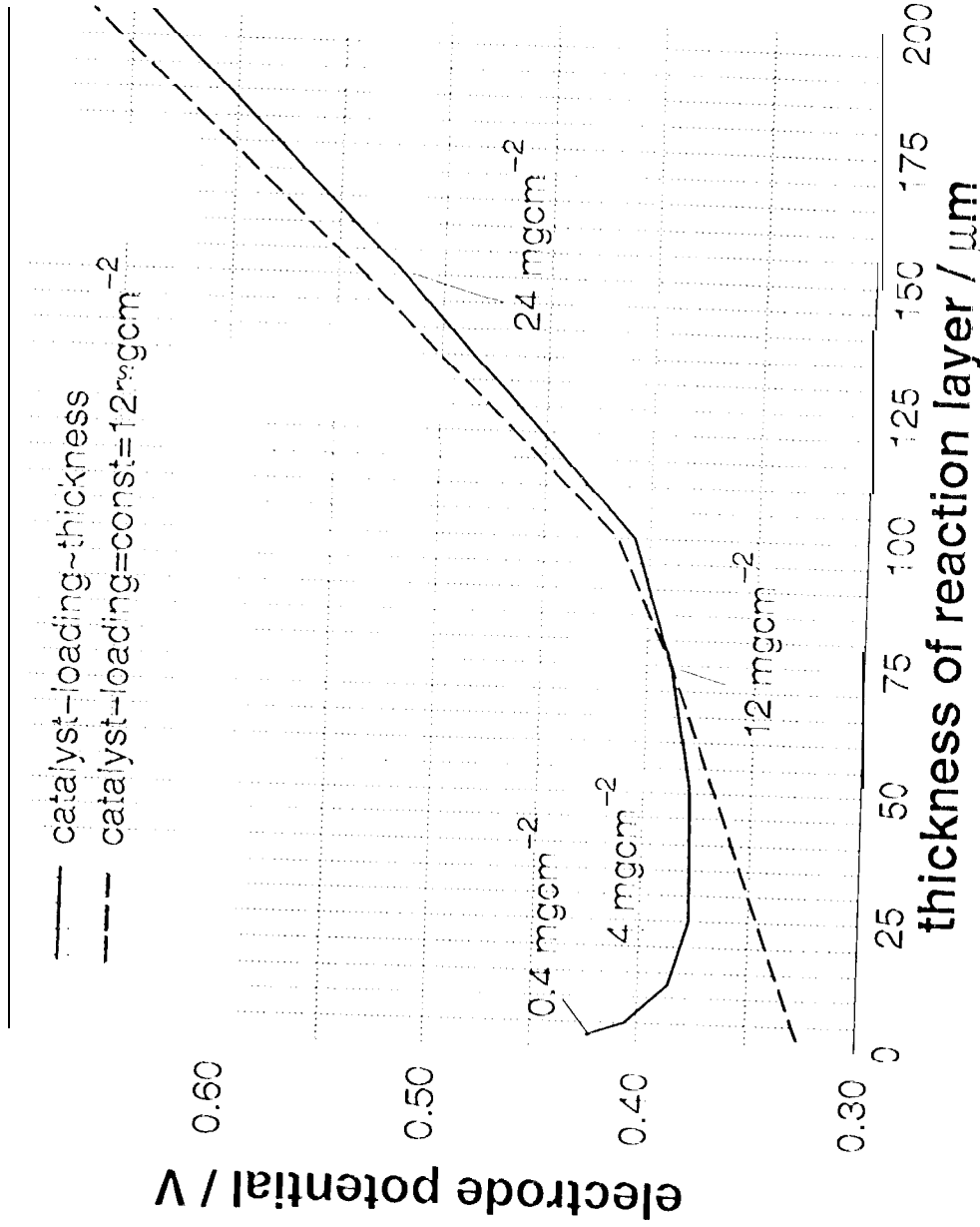
Distribution of methanol concentration in anodic reaction layer



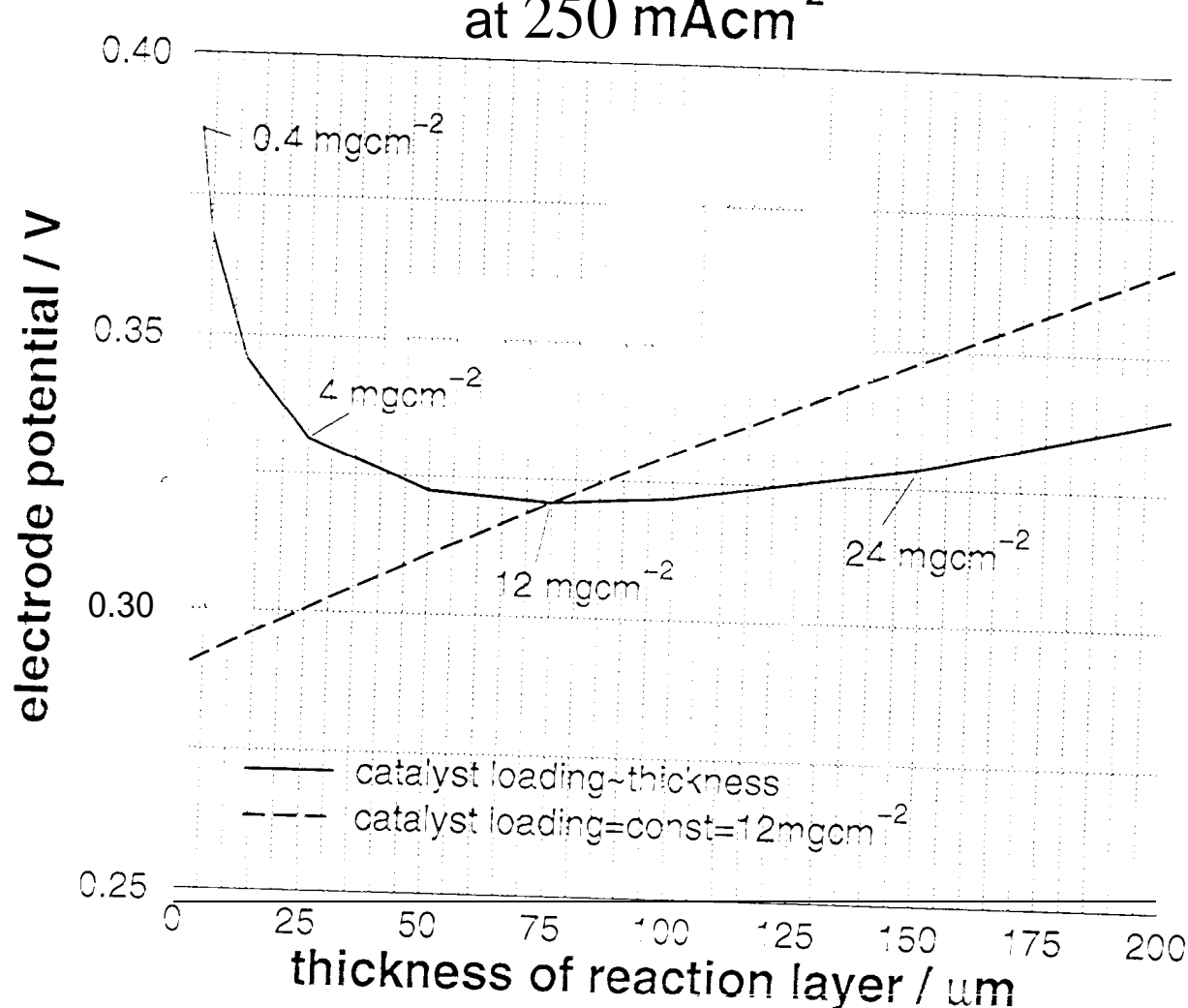
effect of anodic reaction layer thickness on methanol crossover



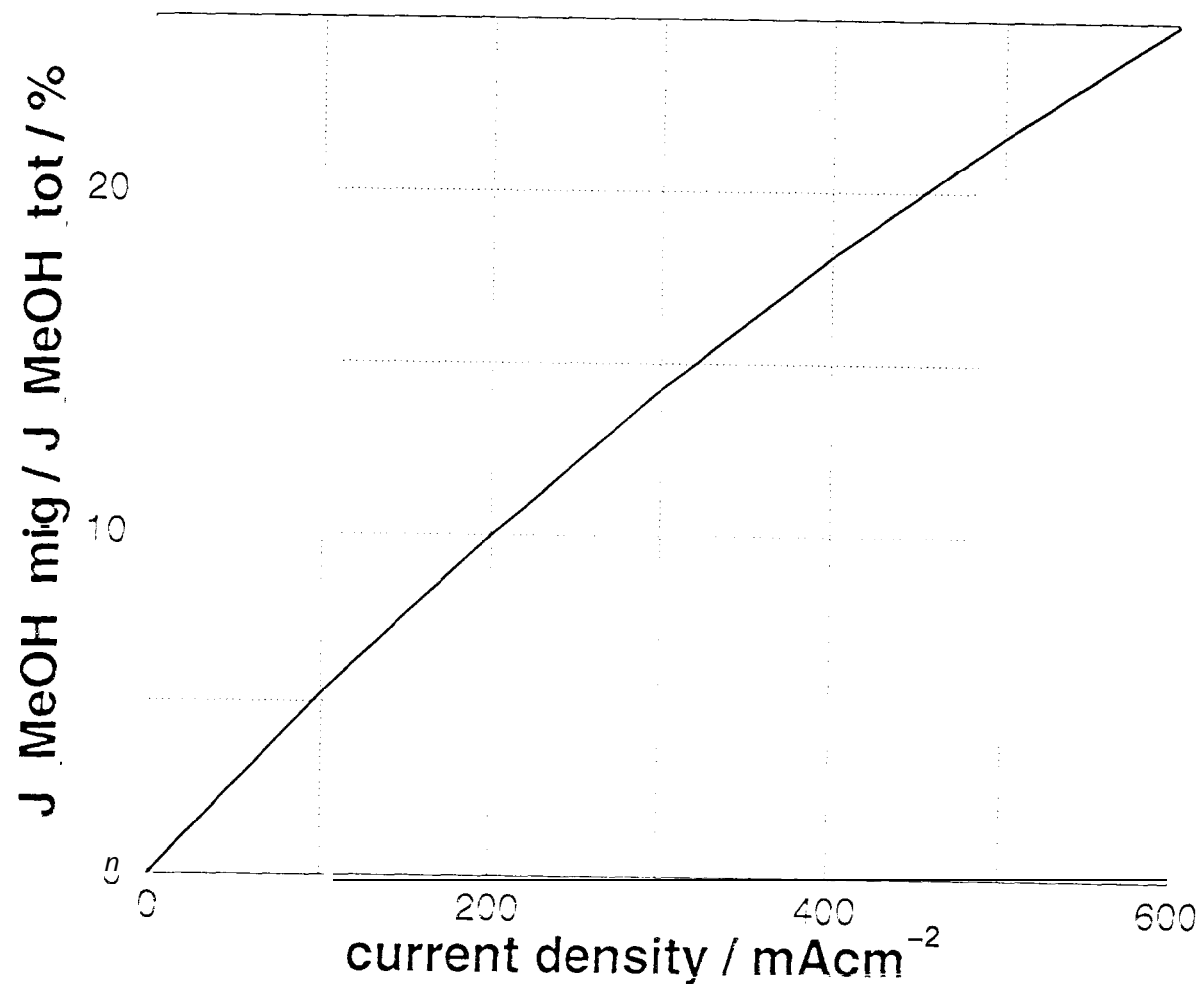
effect of anodic reaction layer thickness on anode potential at 500 mAcm⁻²



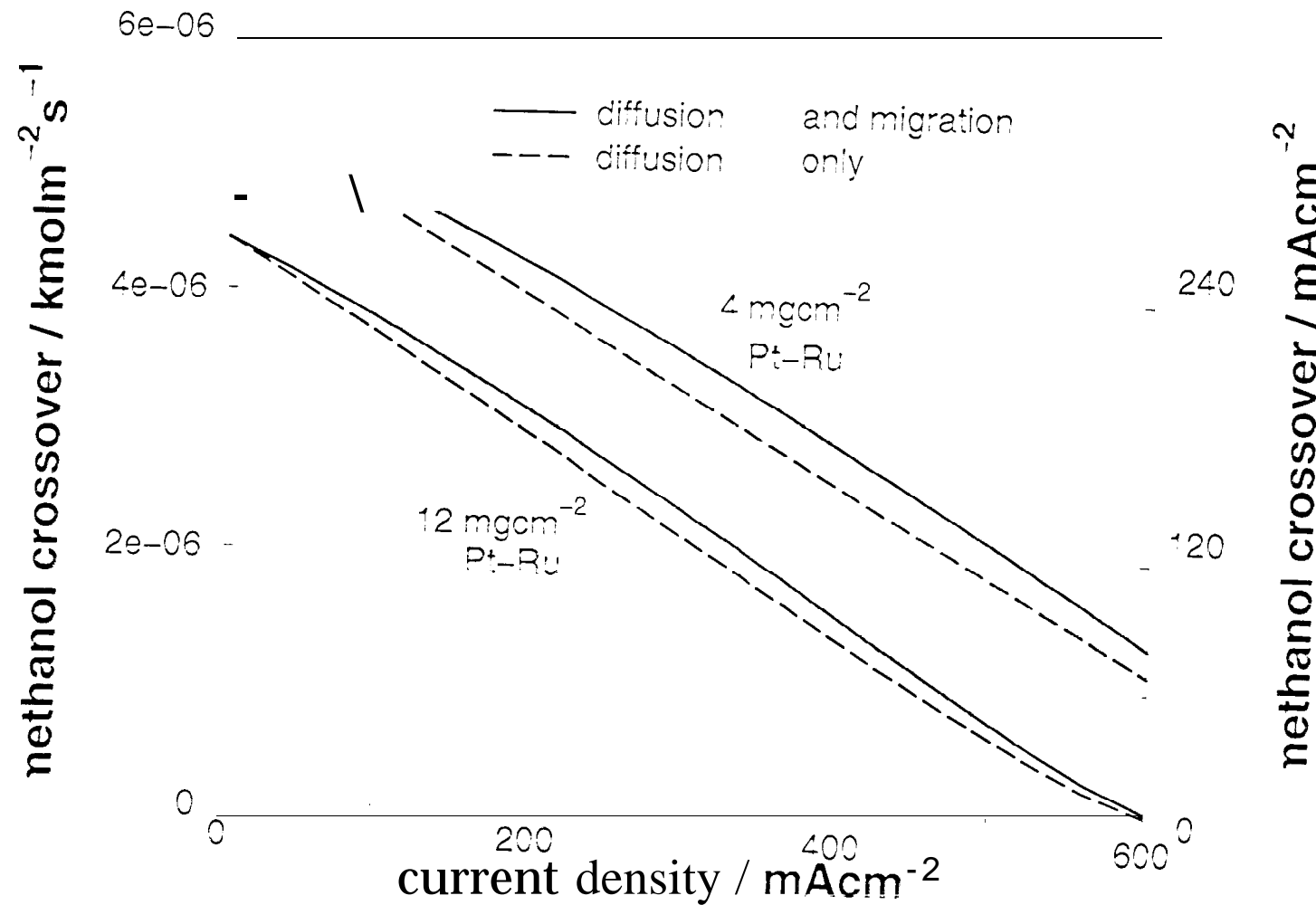
effect of anodic reaction layer thickness on anode potential



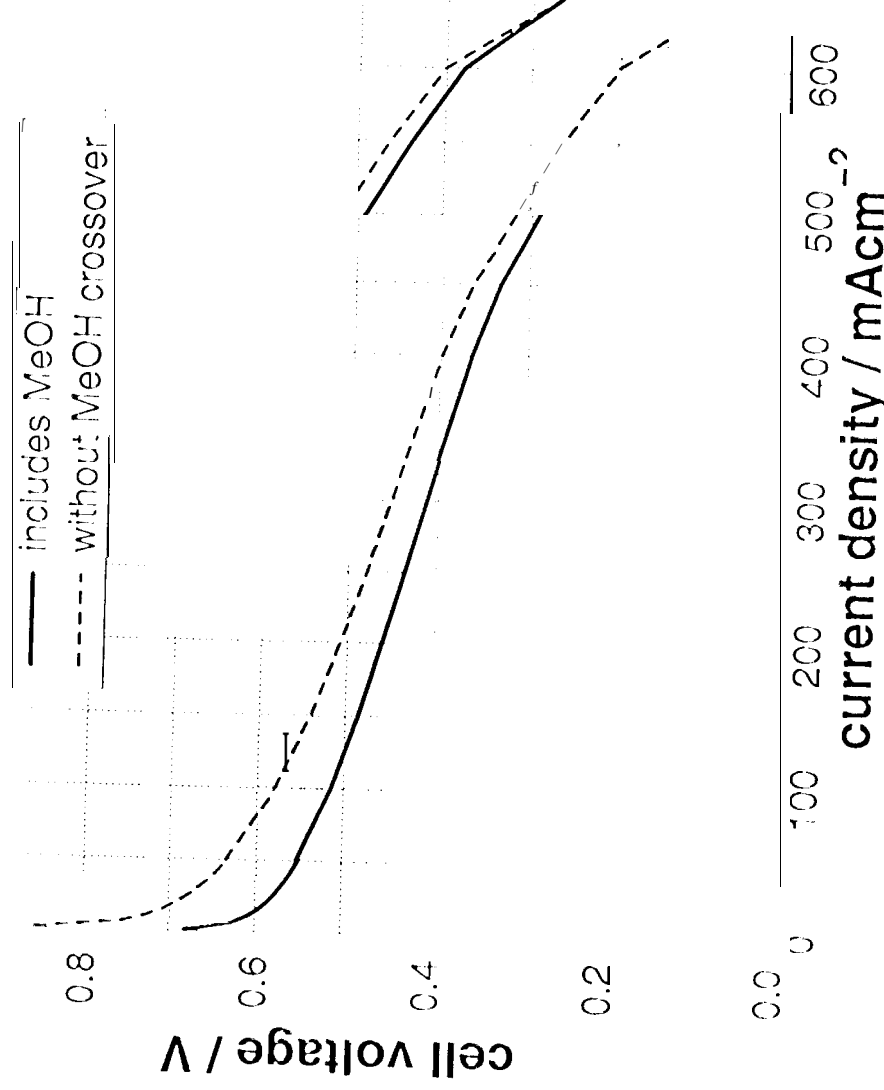
fraction of migration compared to total
methanol crossover rate in Nafion 117 at 90°C



methanol crossover - effect of driving forces



effect of methanol crossover on cell performance (1 M MeOH, 90°C, 20 psig air, 5 l/min)



simulation result of cell performance at 90°C, 20psig air
separation into individual electrode potentials

